Efficient and Robust Coatings Using Poly(2-methyl-2-oxazoline) and Its Copolymers for Marine and Bacterial Fouling Prevention

Tao He,[1] Dominik Jańczewski,[1,2] Satyasankar Jana,[3] Anbanandam Parthiban,[3] Shifeng Guo,[1] Xiaoying Zhu,[1] Serina Siew-Chen Lee,[4] Fernando Jose Parra-Velandia,[4] Serena Lay-Ming Teo,[4] G. Julius Vancso[3,5]

[1]Institute of Materials Research and Engineering, A*STAR (Agency for Science Technology and Research), 3 Research Link, Singapore 117602, Singapore
[2]Laboratory of Technological Processes, Faculty of Chemistry, Warsaw University of Technology, Noakowskiego 3, 00-661, Warsaw, Poland
[3]Institute of Chemical and Engineering Sciences, A*STAR, 1, Pesek Road, Jurong Island, 627833, Singapore
[4]Tropical Marine Science Institute, National University of Singapore, 18 Kent Ridge Road, Singapore, 119227, Singapore
[5]MESA+ Institute for Nanotechnology, Materials Science and Technology of Polymers, University of Twente, P.O. Box 217, 7500 AE, Enschede, The Netherlands
Correspondence to: D. Jańczewski (E-mail: dominik.janczewski@ch.pw.edu.pl) or G. J. Vancso (E-mail: g.j.vancso@utwente.nl)

ABSTRACT: Molecular design, fabrication, and properties of thin-film coatings based on poly(2-methyl-2-oxazoline) (PMOX) and its copolymers were investigated to tackle problem of marine and bacterial fouling prevention. The ultraviolet crosslinkable macromonomer poly(2-methyl-2-oxazoline) dimethylacrylate was synthesized by cationic ring-opening polymerization in a microwave reactor initiated by 1,4-dibromobutane. In order to study the charge effect of the PMOX coatings on the adhesion of fouling organisms, PMOX surfaces with negative, neutral, and positive ζ-potential values were prepared by copolymerization with the positively charged monomer [2-(methacryloyloxy)-ethyl]trimethylammonium chloride. The coatings were stable in sea water for at least 1 month without significant reduction in the film thickness. The marine antifouling activity was evaluated against barnacle cyprids *Amphibalanus amphitrite* and algae *Amphora coffeaeformis*. Results showed that PMOX coatings provide effective reduction of the settlement regardless of the molar mass and surface charge of the polymer. Bacterial adhesion test showed that PMOX coatings effectively reduce *Staphylococcus aureus* and *Escherichia coli* adhesion. Owing to its good stability and antifouling activity PMOX has a great potential as antifouling coating for marine antifouling applications.

KEYWORDS: adhesion; antibacterial; coatings; films; fouling; marine antifouling; polyoxazoline; surface zeta potential; thin polymeric film

INTRODUCTION Marine fouling, defined as unwanted colonization of marine organisms on objects immersed in the sea, can severely damage equipment and structures employed in the maritime industry such as ships, harbor installations, oil rigs, seawater filtration membranes, and pipelines.[1,2] Particularly serious and adverse effects on ships and shipping include increasing fuel consumption, corrosion of ship hulls, and expensive time-consuming maintenance.[3] High-value added, smaller-scale devices such as buoys sensors, and underwater communication equipment are also affected. Recently two preventive approaches have been employed to tackle the marine fouling issue. The first approach is based on the use of biocide-releasing coatings to eradicate or deter fouling species, while the second method aims at utilizing low-adhesive surfaces to prevent initial attachment or to promote fouling release.[4] Wide spread use of biocide-releasing paints however has caused serious environmental damage. Marine biocides were reported to affect marine ecosystems particularly in shallow bays and harbors, where the toxins can easily accumulate.[4] As a result, the use of the most common biocide, tributyl tin (TBT), has been banned by the International Maritime Organization (IMO) since January 2003.[1] In addition, legislative controls in many countries, such as the EU Biocide Products Directive, have resulted in additional restrictions in the use of leachable biocides for marine coatings formulations.[4]

Dedicated to the memory of Professor Edward J. Kramer.

TABLE 1 Synthesis of PMOXDA Polymers

No.	Sample	[monomer]/[initiator]	Yield %	M_w (GPC) g/mol	M_n (GPC) g/mol	PDI[a] (GPC)	DP[b] (NMR)	M_n (NMR) g/mol	F[c] (NMR)
1	$PMOXDA_{5k}$	50	92	7,310	5,150	1.42	62	5,410	1.65
2	$PMOXDA_{3k}$	20	90	4,140	2,800	1.48	34	3,030	1.88

[a] PDI, Polydispersity index.
[b] DP, Degree of polymerization.
[c] *F*, The degree of functionalization (*F*, expressed as the number of acrylate end groups per polymer molecule).

In the battle against marine fouling, non- or low-adhesive coatings are considered as environmentally friendly alternatives.[4] The most commonly used products include nontoxic silicone-based paints, producing hydrophobic surfaces with a low surface energy. As a result, the coated material minimizes the adhesion of the organisms and promotes their detachment at higher water shear rates by the so called fouling release mechanisms.[1,4] Amphiphilic polymer coatings were another type coatings with fouling release properties.[5,6] Highly hydrated, hydrophilic polymer coatings are also among candidates with excellent fouling prevention properties. High-potential materials used to achieve hydration barrier effects[7] include for example zwitterionic polymers[8–10] or polyelectrolyte multilayers.[11,12] Widely investigated poly(ethylene glycol) (PEG) films also demonstrate hydration-related antifouling activity mechanisms.[13,14] It was also generally used as the hydrophilic block in amphiphilic fouling release coatings.[15,16] However, the main weakness of PEG is related to its degradation trough oxidative mechanisms which limit long-term applications. Poly(2-methyl-2-oxazoline) (PMOX) has proven to be a competitive, biocompatible hydrophilic alternative to PEG and has been tested for fouling prevention in biomedical applications.[17–21] One advantage of this polymer is that PMOX is more stable against oxidation than PEG owing to its poly-amide, peptide mimetic chemical structure.[20,22]

Previous antifouling studies using polyoxazolines were mainly directed to the antifouling performance against proteins,[18,20,23] cells,[24] and bacterias.[19,20] To this end, graft copolymers of PMOX with a polycationic backbone composed of poly (L-lysine) (PLL) (PMOX-*g*-PLL) have been used with success. The protecting, PMOX containing films were formed by electrostatic interactions between the positively charged PLL main chains and negatively charged substrate surfaces. Unfortunately, electrostatic interactions can be screened in high ionic strength solutions, such as sea water, leading to desorption of the copolymer and with it the removal of the protecting layer. Unlike the previously described PMOX-*g*-PLL monolayer coatings, the PMOX coatings investigated in this article were fabricated using films covalently bound to the substrates with sufficient thickens to shield the substrate. The covalent linking we used allowed us to assess the efficiency of PMOX as a candidate for a stable marine antifouling material.

EXPERIMENTAL

Materials and Instrumentation

2-Methyl-2-oxazoline (99%, MOX), 1,4-dibromobutane (99%, DBB), acetonitrile (anhydrous, 99.8%, ACN), methanol (anhydrous 99.8%), methacrylic acid (99%, MAA), triethylamine (≥99%, NEt_3), 3-(trimethoxysilyl)propyl methacrylate (MPMS), [2-(methacryloyloxy)ethyl]-trimethylammonium chloride (80 wt % in H_2O, METAC), and diethyl ether (anhydrous, 99%, DEE) were all purchased from Sigma-Aldrich and were used as received.

^1H NMR spectra were recorded on a Bruker 400 MHz spectrometer using the tetramethylsilane signal as a reference. Size exclusion chromatography (SEC) was performed in *N*,*N*-dimethylformamide with one TOSOH H_{HR} Guard Column and one TOSOH GMH_{HR}-M mixed bed column (5 μm, ID 7.8 mm × 300 mm) column and a Viscotek TDA 302 refractive index detector unit. The eluent flow rate was 1.0 mL/min, and the columns were operated at 60 °C. Calibration was conducted with polystyrene. Surface zeta potential (ζ potential) values of the coatings were measured with a SurPASS electrokinetic analyzer from Anton Paar. Thickness of the coatings was obtained using a KLA Tencor P-16+ surface profiler.

Synthesis of Poly(2-methyl-2-oxazoline)-Dimethylacrylate (PMOXDA)

The amounts of MOX and corresponding amounts of the initiator (DBB) were used according to the desired monomer/initiator ratio. In a representative experiment (Table 1, No 2): MOX (70.6 mmol, 6.00 g), DBB (1.4 mmol, 0.31 g), and ACN (8.0 mL) were transferred into a pre-dried microwave vial and placed inside the glovebox used. The vial was capped and placed in the autosampler of the microwave reactor (Biotage® Initiator Classic). After 10 s of pre-stirring, the reaction solutions were heated up to 120 °C and maintained at this temperature for 30 minutes with constant power output of 25 W. Subsequently, the vial was automatically cooled to room temperature by applying nitrogen flow. MAA (5.6 mmol, 0.48 g) was added using a syringe through the septum of the capped microwave vial followed by addition of NEt_3 (5.6 mmol, 0.57 g). The reaction solution was subsequently heated up to 70 °C for 24 h in an oil bath. The resulting product was precipitated in diethyl ether, dried in vacuum and dissolved in methanol followed by precipitation in diethyl ether for two times. After drying in vacuum for 24 h procedure yielded typically 5.80 g of product (yield 92%). ^1H NMR (400 MHz, D_2O): δ (ppm) for $PMOX_{3k}$ 5.99 (s, 0.05H, $=CH_2$), 5.61 (s, 0.05H $=CH_2$); 4.24 (s, 0.11H, CH_2—COO); 3.40 (m, 4H, NCH_2CH_2); 1.97 (m, 3H, $NCOCH_3$); 1.80 (s, 0.17H, $=CCH_3$); 1.52 (b, 0.12H, $NCH_2CH_2CH_2CH_2N$) and for $PMOX_{5k}$ 5.99 (s, 0.02H, $=CH_2$), 5.61 (s, 0.02H, $=CH_2$); 4.24 (s, 0.05H, CH_2—COO); 3.42 (m, 4H, NCH_2CH_2);

1.96 (m, 3H, NCOCH_3); 1.79 (s, 0.09H, =CCH_3); 1.51 (b, 0.07H, NCH_2CH_2CH_2CH_2N). Signal integration normalized for a single repeating unit was performed.

Coating Film Fabrication

Clean silicon wafers were treated with ultraviolet (UV)-Ozone for 30 minutes followed by the vacuum deposition of MPMS at 60 °C for 4 h. PMOXDA was dissolved in methanol at 100 mg/mL with 10 mg/mL of 2-hydroxy-2-methylpropiophenone as photoinitiator. Charge tuning of antifouling films were performed by copolymerization of PMOXDA with the positively charged monomers, METAC. Different amounts of positively charged monomer were added into the PMOXDA solution in order to achieve surfaces with negative, neutral and positive ζ potential. Polymeric films were fabricated by spin-coating at 1000 rpm for 10 s with 100 μL of the solution mixture. After UV-crosslinking for 20 minutes, the surfaces were washed with methanol for 1 minute and subsequently with DI water and artificial sea water for at least 24 h each.

Coatings Characterization

The surface zeta potential (ζ potential) values of the coatings were measured using a SurPASS (Anton Paar) electrokinetic analyzer. Coatings were fabricated on 1 cm × 2 cm silicon slides. Two pieces of such slides were attached to the sample holders and subsequently were inserted into the adjustable gap cell. With the gap height between the slides to be approximately 100 μm, the ζ potential measurement was carried out in 0.001 M KCl water solution and automatic pH titration, in the range 5–10, using 0.05 M NaOH aqueous solution. Because the sample slides were smooth with known surface area, the streaming current mode was used.

Contact angle values were measured using a video contact angle device VCA2500 XE (AST). The static sessile drop method was used. A 2 μL droplet of water was dispensed onto the dry sample surface using a microsyringe and the droplet image was captured 2 minutes later. The image was analyzed by the software provided with the equipment. Six measurements were made for each sample at different locations of their surface.

Stability test of the PMOX coatings were carried out by immersion of the coated substrates into artificial sea water. Upon completion of the immersion period, samples were removed, rinsed with DI water and dried in air. A scratch was made carefully using a sharp needle and the thickness of the coating was measured by a surface profiler (KLA Tencor P-16+).

Bacterial Adhesion Test

Two bacterial strains were used, including *Escherichia coli* (ATCC#: 53868) and *Staphylococcus aureus* (ATTC#: 25923). The two bacterial strains were cultivated in LB broth (10 g of tryptone, 5 g of yeast extract, and 10 g of NaCl) at 37 °C for 16 h before and harvested by centrifuging at 3000 rpm for 10 min. After the removal of the supernatant, the cells were washed twice and re-suspended in PBS. Samples were incubated with bacterial suspensions for 1 h at 37 °C, and then washed three times with PBS before fixing with 3% glutaraldehyde for 5 h at 4 °C. After the fixation, samples were rinsed with DI water to remove the remaining glutaraldehyde, dried at 60 °C for 24 h and imaged with a scanning electron microscope (SEM, JEOL JSM-6360LV). The surface coverage of bacteria was estimated by image analysis of the SEM micrographs using the ImageJ program (available as a public domain Java image processing program provided by National Institute of Health, The United States). The total area covered by the bacteria clusters was divided by the total area of the image to give the percentage coverage of bacteria. Ten images obtained at different locations were used and three samples were measured for each type of surfaces. Bare silicon wafers treated with UV ozone for 30 minutes were used as a reference surface.

Marine Antifouling Test

Amphibalanus amphitrite *Assay*

Barnacle larvae were spawned from adults collected from the Kranji mangrove, Singapore. The nauplius larvae were fed with an algal mixture 1:1 v/v of *Tetraselmis suecica* (CSIRO Strain number CS-187) and *Chaetoceros muelleri* (CSIRO Strain number CS-176) at a density of about 5×10^5 cells/mL, and reared at 27 °C in 2.7% salinity 0.2 μm filtered seawater (FSW). Nauplii metamorphosed into cyprids in 5 days and cyprids were aged for a minimum of 2 days at 4 °C–6 °C before use in the settlement assays.[25] The cyprid settlement assay was carried out using the droplet method.[26] A 300 μL droplet of seawater containing 15–25 cyprids was dispensed onto the modified silica substrate for these tests. The experiment was conducted in the dark at 25 °C for 24 h. After 24 h, the total number of cyprids and the number of settled cyprids were enumerated under an optical microscope. Six replicates were used for every type of sample.

Amphora *Adhesion Assay*

Amphora coffeaeformis (UTEX reference number B2080) was maintained in F/2 medium[27] in tissue culture flasks at 24 °C under a 12 h light and 12 h dark cycle for at least a week prior to use. The algae were gently removed from culture flasks with a cell scrapper and clumps were broken up by continuous pipetting and filtering through a 35 μm nitex mesh. The cell count was determined with a hemocytometer and a suspension containing 10,000 cells/mL was prepared in 3% salinity, 0.22 μm FSW. Sample slides were placed in Nunc® multiwell culture plates, with six replicates for each sample. About 5 mL of algal cell suspension was added into every well. The culture plates were incubated for 24 h in 12 h light and 12 h dark cycle at 24 °C. At the end of the incubation, all slides were gently rinsed with FSW to remove any unattached cells. After drying in air, the slides were examined under an epi-fluorescence microscope. Ten random fields of views were counted at 20× magnifications for each slide. Every field of view had an area of 0.916 mm^2. Bare silicon wafers treated with UV ozone were used as a control for the antifouling tests.

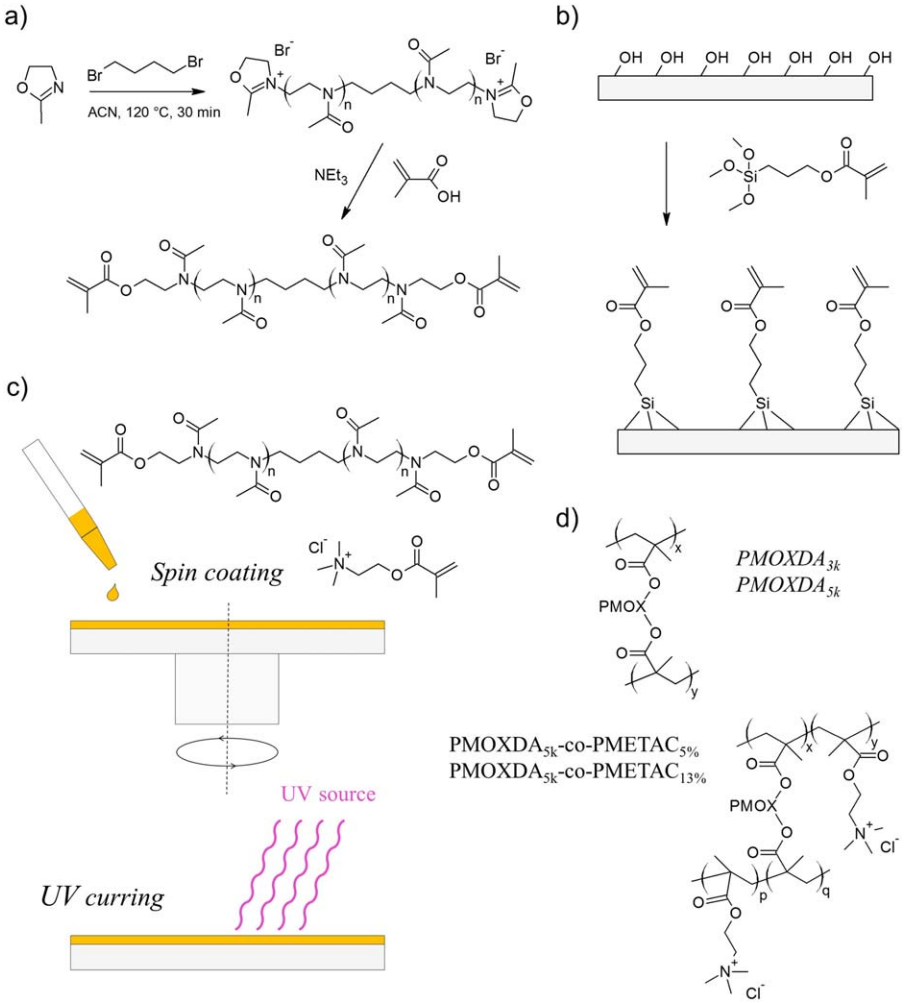

SCHEME 1 (a) Living cationic ROP of 2-methyl-2-oxazoline initiated by 1,4-dibromobutane and end capping with methacrylic acid; (**b**) Silane treatment of Si wafer; (**c**) Film fabrication by spin coating and UV crosslinking; (**d**) Chemical structure of the crosslinked films.

RESULTS AND DISCUSSION

The schematics of the synthesis and preparation of the coatings are shown in Scheme 1. Explanation of the different steps follows below.

Synthesis of PMOXDA

The macro-monomer PMOXDA (see Scheme 1) was synthesized by living cationic ring-opening polymerization (ROP) of 2-methyl-2-oxazoline initiated by 1,4-dibromobutane and terminated by addition of methacrylic acid [Scheme 1(a)]. 2-Methyl-oxazoline was polymerized in acetonitrile at 120 °C under microwave irradiation in the presence of varying amounts of the initiator in order to control the chain length. End capping reaction of the living oxazolinium species with methacrylic acid was carried out in the presence of a proton scavenger NEt_3. The synthetic methodology was inspired by the approach of Christova et al.,[28] but rather than employing a conventional heating method, a microwave reactor was used in our study following the procedure described by the Schubert group.[29,30] Instead of the alkene initiator used in previous studies, 1,4-dibromo-2-butane, a simple alkyl bromide without iodized salt as a catalyst was applied for the first time to initiate oxazoline polymerization. Typical initiators for oxazoline ROP include methyl triflate (MeOTf), methyl tosylate (MeOTs), acetyl halide, and alkyl halide.[31–39] Lower nucleophilicity of the counterion leads to higher polymerization rates.[32] MeOTf or MeOTs have higher initiation rates but display elevated sensitivity to residual moisture and other small contaminations resulting in the loss of control over the process.[32] When alkyl halide was used as the initiator, iodized salt was required as catalyst except for alkyl iodide and benzyl halide.[34,35,37,40] In the process proposed in this article the simple alkyl bromide, 1,4-dibromobutane, was used successfully as initiator without iodized salts, thanks to application of the microwave activation support.

Two PMOXDA polymers characterized by different molar masses were synthesized as shown in Table 1. In both cases, the polymer yields were close to quantitative. Owing to the

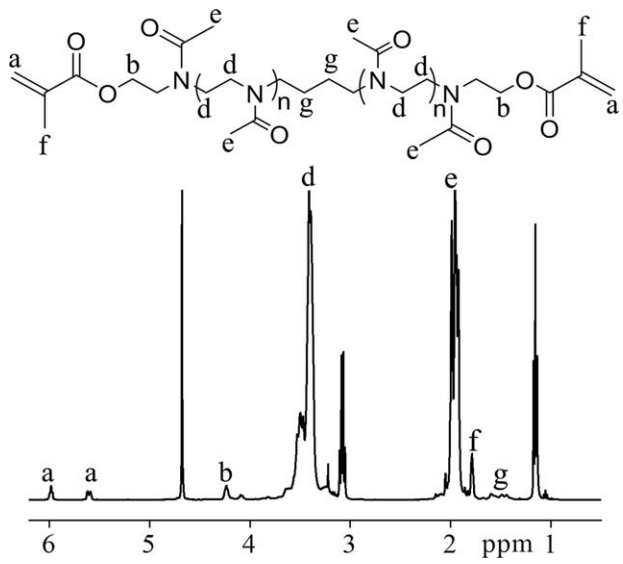

FIGURE 1 ^{1}H NMR spectrum (400 MHz, solvent D_2O) of $PMOXDA_{3K}$.

use of the high temperature and high-pressure in the microwave reactor, and to the fast, selective non-contact heating by the microwave irradiation, the reaction time of the polymerization was reduced to 30 minutes which was several hours shorter than for conventional heating methods.[33] The average degree of polymerization was calculated by comparing the integrated areas of the NMR signals of the initiator fragments in the chain —$CH_2CH_2CH_2CH_2$— at 1.5 ppm to the integrated areas of the polymer backbone peaks —CH_2CH_2N— at 3.40 ppm (Fig. 1). As shown in Table 1, M_n values of the polymer determined by GPC were in good agreement with values obtained by NMR. The polymers displayed polydispersity indices (PDI) less than 1.5. One may note that PDI of our product was slightly higher than reported typical narrow distribution values, which are normally less than 1.2 for microwave reactions.[33] This may be associated with the initiator used for our process which has lower activity of initiation as compared with benzyl or allyl halides; however, a direct comparison is problematic since no purification and drying of the monomer and solvent were performed in our study. The impurities may induce chain transfer side reactions leading to the higher polydispersity and also lower end-group functionalization. The degree of functionalization (F), describing the number of acrylate end groups per polymer molecule, was established as 1.65 for $PMOXDA_{5K}$ and 1.88 for $PMOXDA_{3K}$, using the ratio of the peak areas obtained by NMW of the initiator fragment (1.52 ppm) and hydrogens next to the acrylate groups —COO—CH_2— (4.24 ppm).

Coating Preparation and Characterization

The Si substrates were treated with MPMS in order to covalently bond the PMOX coatings as shown in Scheme 1(b). The successful modification was confirmed by an increase of contact angle value from less than 5° for bare Si to 60° after deposition. To investigate the properties of the antifouling films, coatings of PMOX with well-controlled thickness values were fabricated by spin coating, followed by UV light cross-linking, as shown in Scheme 1(c,d). Since most of the foulants are charged, electrostatic interactions between these charged species and the polymer films play an important role in the fouling processes, particularly during the initial adsorption stage.[11,41,42] We complemented the synthesis of our PMOX films by addition of positively charged monomers to control the ζ potential of the coating films. ζ potential versus pH was measured by streaming potential experiments and the results obtained are shown in Figure 2.

The positively charged monomer METAC was copolymerized with the PMOXDA macromonomers as shown in Scheme 1(c) and Table 2. Addition of 5% of METAC (mass percentage of METAC to PMOXDA) yielded a neutral ζ-potential for PMOXDA-*co*-$PMETAC_{5\%}$ at pH 8. Further increase of the METAC to 13% leads to a positively charged surface PMOXDA-*co*-$PMETAC_{13\%}$ with a ζ-potential value of +34 mV at pH 8. It was particularly important to fabricate surface displaying neutral character at pH 8, as this constitutes typical environmental conditions in seawater.[43] Pure PMOX films constructed in our study ($PMOXDA_{5K}$ and $PMOXDA_{3K}$) displayed negative ζ-potentials in the range of −30 to −25 mV, despite lack of formal charges in the molecule structure. Typically, the negative ζ-potential is seen at the surface owing to the specific affinity of anions to a polymeric material. This effect was broadly discussed for many polymers,[44–46] and is most likely also responsible for the observed negative ζ-potentials of the PMOX films.

As shown in Table 2, all our coated surfaces displayed similar contact angle values of around 25°–30°. These values correspond well to the reported values of PMOX materials.[36] PMOX is considered to be a hydrophilic polymer similar to PEG, thus the relatively low contact angle was expected.[20,47] The dry thickness of all four coatings after UV irradiation was 1.1 μm before washing with methanol and DI water. The thickness values were decreased after washing off the

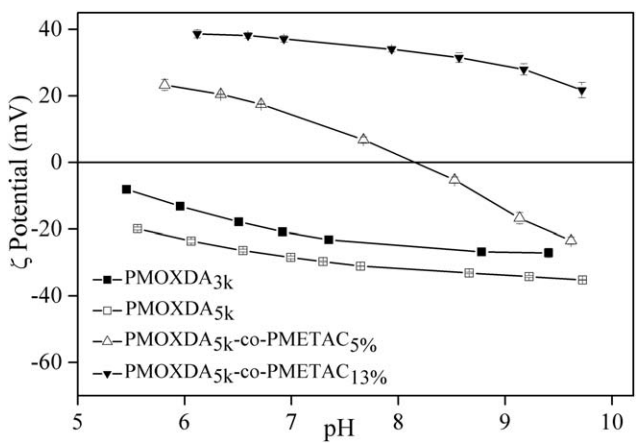

FIGURE 2 ζ-potential of different coatings versus pH. Error bars correspond to standard deviations.

TABLE 2 Film Composition, and ζ-Potential, Contact Angle, and Thickness Values for Different Coatings

Sample	$PMOXDA_{3k}$	$PMOXDA_{5k}$	$PMOXDA_{5k}$-*co*-$PMETAC_{5\%}$	$PMOXDA_{5k}$-*co*-$PMETAC_{13\%}$
PMOXDA concentration (mg/mL)	100	100	100	100
METAC (mg/mL)	0	0	5	13
Film ζ-potential at pH = 8 (mV)	−24	−32	0	+34
Film contact angle (°)	25 ± 3	28 ± 3	27 ± 2	32 ± 4
Film thickness (nm)	332 ± 22	231 ± 15	230 ± 13	200 ± 14

uncrosslinked top material which was the oxygen inhibition layer formed during the free radical UV curing of the acrylate group.[48] Following washing, the observed thickness of $PMOXDA_{3k}$ was 332 ± 22 nm, which was 100 nm thicker than $PMOXDA_{5k}$. This difference could be linked to the faster crosslinking kinetics because of higher molar concentration of the acrylate end groups at the same mass concentration of polymer for $PMOXDA_{3k}$. During the UV crosslinking, the methanol gradually evaporates and the oxygen can penetrate into the coatings. Once oxygen is present, the crosslinking reaction is inhibited and uncrosslinked layers can be formed. Obviously, faster crosslinking reactions result in thinner oxygen inhibition layers; in other words yield thicker coatings after removing the non-bounded layer.

In order to assess the applicability of the coatings described, thickness values of the coatings immersed in artificial sea water were measured as a function of exposure time. The medium used is considered a highly corrosive environment.[49] The results for four coatings are displayed in Figure 3. After 60 days of immersion, all coatings were intact. After the initial faster loss in the film thickness, which can be associated with the removal of the loosely bound material, the thickness remained constant at above 80% of its original value. These results confirm good stability of PMOX coatings in artificial sea water for long-term applications.

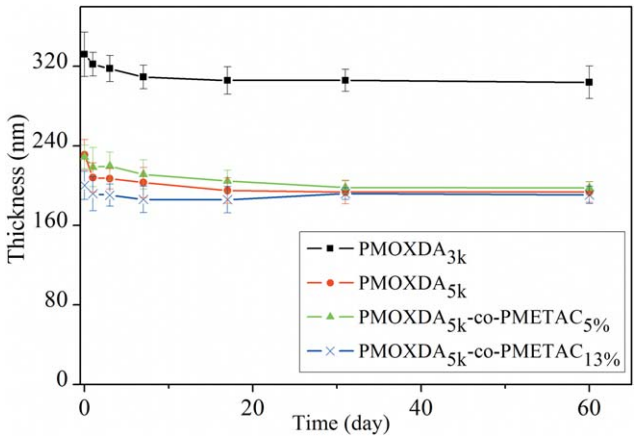

FIGURE 3 Coating thickness versus time of the different surfaces (composition and explanation of symbols are shown in the inset) as measured by surface profiler. Error bars correspond to standard deviations.

Bacterial Adhesion Test

Since bacterial fouling is particularly relevant for biomedical applications, two common bacteria living in the physiological environment and cultured in PBS, that is, *E. coli* (Gram negative) and *S. aureus* (Gram positive) were used to test PMOX coatings. Bacterial coverage was evaluated using image analysis of SEM pictures taken from substrates samples exposed to the bacterial suspension for 1-h period.

Bacterial surfaces are negatively charged due to ionized phosphoryl and carboxylate substituent's on the outer cell envelope.[50] Thus, the adhesion of bacteria on the control (S1) was very low (coverage 1.4% ± 0.4% for *S. aureus* and 0.4% ± 0.1% for *E. coli*) owing to the strong negative charge and strong hydrophilicity of the silanol groups present at the freshly cleaned silicon wafer surface. The adhesion on the plain PMOX coating without adding positively charged monomer remained at the same (or lower) level [0.5% ± 0.1% and 0.3% ± 0.3% for *E. coli* on $PMOXDA_{3K}$ (S2) and $PMOXDA_{5K}$ (S3); coverage 0.1% ± 0.1% and 0.1% ± 0.1% for *S. aureus* on $PMOXDA_{3K}$ (S2) and $PMOXDA_{5K}$ (S3)]. The results are consistent with a previous study of the antifouling performance of PMOX-*g*-PLL graft copolymers using bacteria.[19] A clear tendency in increase of the bacterial adhesion could be observed when the ζ-potential was shifting from negative to positive values. For the $PMOXDA_{5k}$-*co*-$PMETAC_{5\%}$ (S4) surface, which is slightly positively charged at pH 7.4, the coverage of *S. aureus* and *E. coli* increased to 1.2% ± 0.4% and 5.4% ± 2.0%, respectively. For $PMOXDA_{5k}$-*co*-$PMETAC_{13\%}$ (S5), surface with higher positive ζ-potential, the bacterial coverage increased further to 6.6% ± 1.8% and 18.0% ± 1.6% for the *S. aureus* and *E. coli,* respectively. This clearly indicates that positive potentials deteriorate the antifouling performance of PMOX toward bacteria. Similar results on the charge effect on bacterial adhesion has been found in our recent study based on layer-by-layer assembled, charged polyelectrolyte multilayer systems (Fig. 4).[11]

Antifouling Activity against Marine Organisms

The marine antifouling activity of the coatings was tested against cyprids (larvae of the barnacle *Amphibalanus amphitrite*) and algae *Amphora coffeaeformis* as shown in Figure 5.

The cyprid larva is the last larval stage of the barnacle metamorphotic cycle. At this stage of development, the animal is exploring surfaces to find a suitable place to settle.[51] As shown in Figure 5(a), cyprids settlement (percentage of

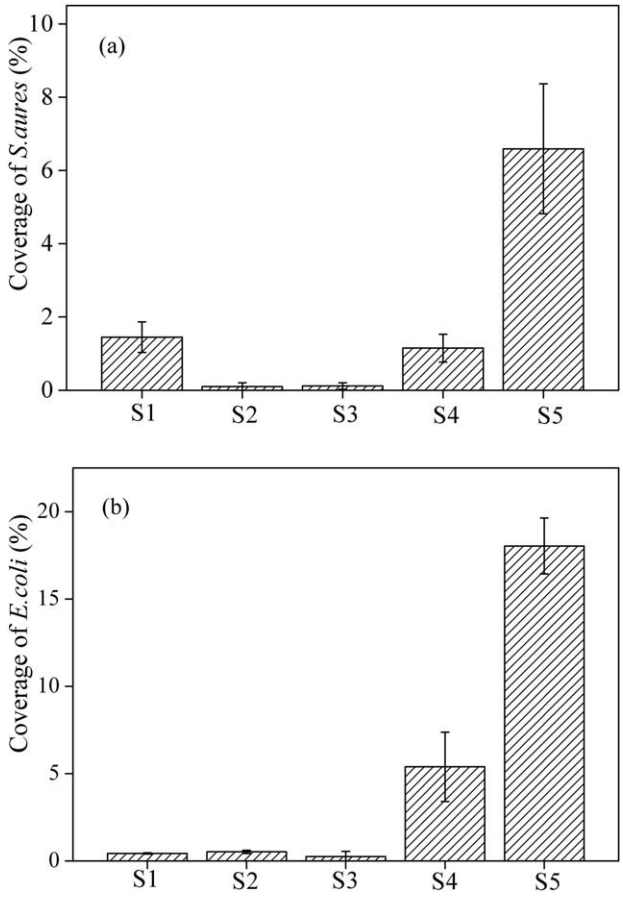

FIGURE 4 Bacteria coverage on different coating surfaces of (**a**) *S. aureus,* (**b**) *E. coli* adhesion assays. Error bars correspond to the standard deviations. S1:Si; S2:PMOXDA$_{3k}$; S3:PMOXDA$_{5k}$; S4:PMOXDA$_{5k}$-*co*-PMETAC$_{5\%}$; S5: PMOXDA$_{5k}$-*co*-PMETAC$_{13\%}$.

settled organisms divided by the total number of cyprids used) was significantly reduced on all PMOX coated surfaces regardless of the polymer molar mass or surface charge (One-way ANOVA test, $p < 0.05$). The settlement on clean silicon wafers (S1) was close to 50% while for all four PMOX coated samples it was less than 3% with no significant difference between the specimens (student's *t*-test, $p < 0.05$). Another investigated species, *Amphora coffeaeformis,* is the most commonly encountered raphid-diatom found in biofilms on submerged surfaces and as such, is often used in antifouling tests.[52] After incubation in the *Amphora* suspension, the surfaces were investigated with fluorescence microscopy, and the number of attached *Amphora* cells was scored. As shown in Figure 5(b), about 82 ± 10 cells/mm^2 were observed on the control surface (bare silicon wafer, S1) which was significantly higher than all four PMOX coated surfaces (One-way ANOVA test, $p < 0.05$). In other words, PMOX coatings effectively reduced *Amphora* settlement. There was no difference between PMOXDA$_{3k}$ (S2) and PMOXDA$_{5k}$ (S3) with 46 ± 12 and 44 ± 11 cells/mm^2 though the molar mass of PMOXDA$_{3k}$ was half of PMOXDA$_{5k}$. PMOXDA$_{5k}$-*co*-PMETAC$_{13\%}$ (S5) with a positive ζ-potential yielded a settlement density at 58 ± 13 cells/mm^2 which was slightly higher than PMOXDA$_{5k}$ with negative ζ-potential (S3) but the difference is not significant (student's *t*-test, $p > 0.05$).

The antifouling activity of PMOX is associated with its hydrophilicity.[20] The highly hydrated structures help to resist both the adhesion of cyprids as well as *Amphora*, however coatings were more effective against barnacles then for algae. Tightly bound water molecules form a physical hydration barrier and prevent nonspecific foulant adhesion.[8,53,54] Similar marine antifouling phenomena have been reported for other highly hydrated systems, such as polyelectrolyte multilayers[12] and PEG containing hydrogels.[13,14] The surface charge is one of the key parameters that affects the adhesion of foulants and it has been reported that cyprids avoid settlement on positively charged surfaces.[11,42] However, in our research, no further reduction of the settlement on the positively charged PMOXDA$_{5k}$-*co*-PMETAC$_{13\%}$ (S5) surface could be observed as compared with negatively charged PMOXDA$_{5k}$ (S3). We speculate that owing to the very low settlement on PMOX coating itself and to the relatively large variation of the data, no significant difference could be seen in PMOX samples with various densities of surface charge. Reduction in the amphora settlement was also significant when

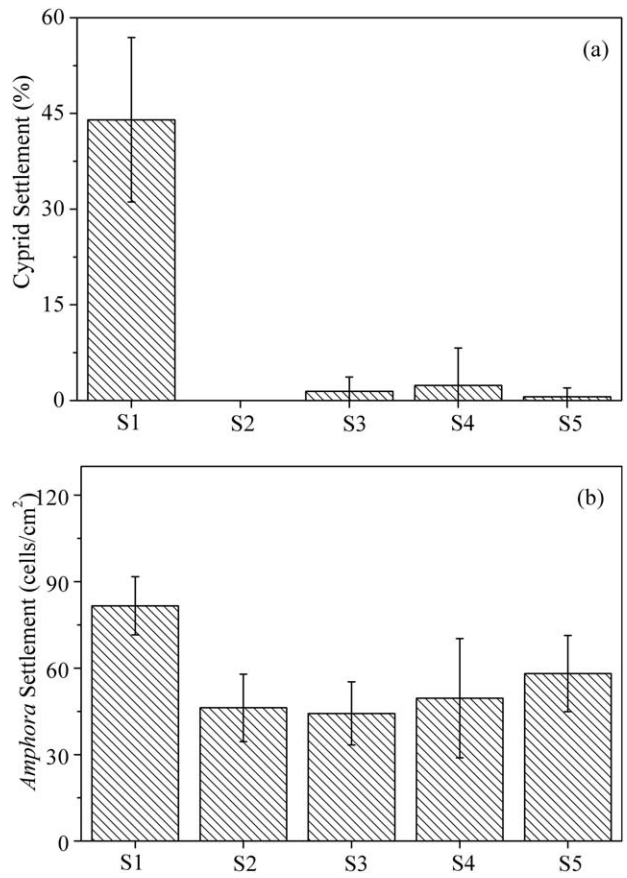

FIGURE 5 (a) Cyprids of *Amphibalanus amphitrite* and (**b**) *Amphora coffeaeformis* settlement on different surface. Error bars correspond to the standard deviations. S1:Si; S2:PMOXDA$_{3k}$; S3:PMOXDA$_{5k}$; S4:PMOXDA$_{5k}$-*co*-PMETAC$_{5\%}$; S5: PMOXDA$_{5k}$-*co*-PMETAC$_{13\%}$.

compared with Si surfaces. The adhesion of amphora on different PMOX coating was not affected by the surface ζ-potential. This result was consistent with our previous study on the charged LbL multilayer surface concluding that *Amphora* does not respond to variations of surface charge.[11]

CONCLUSIONS

PMOXDA macromonomers with methyl acrylate end groups were successfully synthesized via a living cationic ROP using a novel type of initiator in combination with microwave assisted synthesis, substantially broadening the available initiators for this type of reaction. Thin PMOX films were fabricated by spin coating, followed by a UV crosslinking of the methyl acrylate end group. The tuning of the electrostatic charge was achieved by copolymerization with different amounts of a positively charged monomer added to the spin coating solution. The covalently crosslinked and thick PMOX coatings showed great stability in artificial sea water and were good model surfaces to assess the antifouling activity of PMOX. The marine antifouling activity of PMOX coatings was confirmed against two marine organisms for the first time. The settlement of *Barnacles* and *Amphor*a on all PMOX coated surfaces was successfully reduced regardless of the surface ζ-potential. The charge effect was, however, very obvious for bacterial adhesion. The results showed that PMOX coatings effectively reduce *S. aureus* and *E. coli* adhesion, however, the incorporation of positive charge may lead to deterioration of the layer performance. We believe this work can help to pave the way for using the PMOX as antifouling material especially for marine antifouling applications.

ACKNOWLEDGMENTS

The authors are grateful to the Agency for Science, Technology and Research (A*STAR) for providing financial support under the Innovative Marine Antifouling Solutions (IMAS) program.

REFERENCES AND NOTES

1 D. M. Yebra, S. Kiil, K. Dam-Johansen, *Prog. Org. Coat.* **2004**, *50*, 75–104.

2 J. A. Callow, M. E. Callow, *Nat. Commun.* **2011**, *2*, 244.

3 M. P. Schultz, J. A. Bendick, E. R. Holm, W. M. Hertel, *Biofouling* **2011**, *27*, 87–98.

4 M. Lejars, A. Margaillan, C. Bressy, *Chem. Rev.* **2012**, *112*, 4347–4390.

5 S. Krishnan, R. Ayothi, A. Hexemer, J. A. Finlay, K. E. Sohn, R. Perry, C. K. Ober, E. J. Kramer, M. E. Callow, J. A. Callow, D. A. Fischer, *Langmuir* **2006**, *22*, 5075–5086.

6 W. van Zoelen, H. G. Buss, N. C. Ellebracht, N. A. Lynd, D. A. Fischer, J. Finlay, S. Hill, M. E. Callow, J. A. Callow, E. J. Kramer, R. N. Zuckermann, R. A. Segalman, *ACS Macro Lett.* **2014**, *3*, 364–368.

7 S. F. Chen, L. Y. Li, C. Zhao, J. Zheng, *Polymer* **2010**, *51*, 5283–5293.

8 W. J. Yang, K. G. Neoh, E. T. Kang, S. S. C. Lee, S. L. M. Teo, D. Rittschof, *Biofouling* **2012**, *28*, 895–912.

9 R. Quintana, D. Jańczewski, V. A. Vasantha, S. Jana, S. S. C. Lee, F. J. Parra-Velandia, S. Guo, A. Parthiban, S. L. M. Teo, G. J. Vancso, *Colloid Surf. B* **2014**, *120*, 118–124.

10 Z. Zhang, J. A. Finlay, L. F. Wang, Y. Gao, J. A. Callow, M. E. Callow, S. Y. Jiang, *Langmuir* **2009**, *25*, 13516–13521.

11 X. Y. Zhu, D. Jańczewski, S. F. Guo, S. S. C. Lee, F. J. P. Velandia, S. L. M. Teo, T. He, S. R. Puniredd, G. J. Vancso, *ACS Appl. Mater. Interfaces* **2015**, *7*, 852–861.

12 X. Y. Zhu, D. Jańczewski, S. S. C. Lee, S. L. M. Teo, G. J. Vancso, *ACS Appl. Mater. Interfaces* **2013**, *5*, 5961–5968.

13 T. Ekblad, G. Bergstroem, T. Ederth, S. L. Conlan, R. Mutton, A. S. Clare, S. Wang, Y. Liu, Q. Zhao, F. D'Souza, G. T. Donnelly, P. R. Willemsen, M. E. Pettitt, M. E. Callow, J. A. Callow, B. Liedberg, *Biomacromolecules* **2008**, *9*, 2775–2783.

14 P. Lundberg, A. Bruin, J. W. Klijnstra, A. M. Nystrom, M. Johansson, M. Malkoch, A. Hult, *ACS Appl. Mater. Interfaces* **2010**, *2*, 903–912.

15 Y. Cho, H. S. Sundaram, J. A. Finlay, M. D. Dimitriou, M. E. Callow, J. A. Callow, E. J. Kramer, C. K. Ober, *Biomacromolecules* **2012**, *13*, 1864–1874.

16 M. D. Dimitriou, Z. Zhou, H. S. Yoo, K. L. Killops, J. A. Finlay, G. Cone, H. S. Sundaram, N. A. Lynd, K. P. Barteau, L. M. Campos, D. A. Fischer, M. E. Callow, J. A. Callow, C. K. Ober, C. J. Hawker, E. J. Kramer, *Langmuir* **2011**, *27*, 13762–13772.

17 O. Sedlacek, B. D. Monnery, S. K. Filippov, R. Hoogenboom, M. Hruby, *Macromol. Rapid Commun.* **2012**, *33*, 1648–1662.

18 R. Konradi, B. Pidhatika, A. Muhlebach, M. Textor, *Langmuir* **2008**, *24*, 613–616.

19 B. Pidhatika, J. Moller, E. M. Benetti, R. Konradi, E. Rakhmatullina, A. Muhlebach, R. Zimmermann, C. Werner, V. Vogel, M. Textor, *Biomaterials* **2010**, *31*, 9462–9472.

20 R. Konradi, C. Acikgoz, M. Textor, *Macromol. Rapid Commun.* **2012**, *33*, 1663–1676.

21 L. Tauhardt, K. Kempe, M. Gottschaldt, U. S. Schubert, *Chem. Soc. Rev.* **2013**, *42*, 7998–8011.

22 B. Pidhatika, M. Rodenstein, Y. Chen, E. Rakhmatullina, A. Muhlebach, C. Acikgoz, M. Textor, R. Konradi, *Biointerphases* **2012**, *7*, 1.

23 H. Wang, L. Li, Q. Tong, M. Yan, *ACS Appl. Mater. Interfaces* **2011**, *3*, 3463–3471.

24 N. Zhang, T. Pompe, I. Amin, R. Luxenhofer, C. Werner, R. Jordan, *Macromol. Biosci.* **2012**, *12*, 926–936.

25 P. R. Willemsen, K. Overbeke, A. Suurmond, *Biofouling* **1998**, *12*, 133–147.

26 J. A. Finlay, S. M. Bennett, L. H. Brewer, A. Sokolova, G. Clay, N. Gunari, A. E. Meyer, G. C. Walker, D. E. Wendt, M. E. Callow, J. A. Callow, M. R. Detty, *Biofouling* **2010**, *26*, 657–666.

27 R. R. Guillard, J. H. Ryther, *Can. J. Microbiol.* **1962**, *8*, 229–239.

28 D. Christova, R. Velichkova, E. J. Goethals, *Macromol. Rapid Commun.* **1997**, *18*, 1067–1073.

29 F. Wiesbrock, R. Hoogenboom, C. H. Abeln, U. S. Schubert, *Macromol. Rapid Commun.* **2004**, *25*, 1895–1899.

30 C. Weber, C. R. Becer, R. Hoogenboom, U. S. Schubertt, *Macromolecules* **2009**, *42*, 2965–2971.

31 R. M. Paulus, C. R. Becer, R. Hoogenboom, U. S. Schubert, *Macromol. Chem. Phys.* **2008**, *209*, 794–800.

32 R. Hoogenboom, M. W. M. Fijten, U. S. Schubert, *J. Polym. Sci. Part A: Polym. Chem.* **2004**, *42*, 1830–1840.

33 F. Wiesbrock, R. Hoogenboom, M. A. M. Leenen, M. A. R. Meier, U. S. Schubert, *Macromolecules* **2005**, *38*, 5025–5034.

34 J. Y. Yuan, N. ten Brummelhuis, M. Junginger, Z. L. Xie, Y. Lu, A. Taubert, H. Schlaad., *Macromol. Rapid Commun.* **2011**, *32*, 1157–1162.

35 J. Rueda, S. Zschoche, H. Komber, D. Schmaljohann, B. Voit, *Macromolecules* **2005**, *38*, 7330–7336.

36 N. Zhang, M. Steenackers, R. Luxenhofer, R. Jordan, *Macromolecules* **2009**, *42*, 5345–5351.

37 G. Volet, V. Chanthavong, W. Wintgens, C. Amiel, *Macromolecules* **2005**, *38*, 5190–5197.

38 B. Guillerm, S. Monge, V. Lapinte, J. J. Robin, *Macromolecules* **2010**, *43*, 5964–5970.

39 M. Glassner, D. R. D'Hooge, J. Y. Park, P. H. M. Van Steenberge, B. D. Monnery, M. F. Reyniers, R. Hoogenboom, *Eur. Polym. J.* **2015**, *65*, 298–304.

40 M. W. M. Fijten, R. Hoogenboom, U. S. Schubert, *J. Polym. Sci. Part A: Polym. Chem.* **2008**, *46*, 4804–4816.

41 P. O. Glantz, T. Arnebrant, T. Nylander, R. E. Baier, *Acta Odontol. Scand.* **1999**, *57*, 238–241.

42 L. Petrone, A. D. Fino, N. Aldred, P. Sukkaew, T. Ederth, A. S. Clare, B. Liedberg, *Biofouling* **2011**, *27*, 1043–1055.

43 P. J. Hansen, *Aquat. Microb. Ecol.* **2002**, *28*, 279–288.

44 R. Zimmermann, U. Freudenberg, R. Schweiss, D. Kuettner, C. Werner, *Curr. Opin. Colloid Interface Sci.* **2010**, *15*, 196–202.

45 K. Emoto, Y. Nagasaki, K. Kataoka, *Langmuir* **1999**, *15*, 5212–5218.

46 C. S. Tian, Y. R. Shen, *Proc. Natl. Acad. Sci. USA* **2009**, *106*, 15148–15153.

47 N. Adams, U. S. Schubert, *Adv. Drug Deliv. Rev.* **2007**, *59*, 1504–1520.

48 A. K. O'Brien, C. N. Bowman, *Macromol. Theor. Simul.* **2006**, *15*, 176–182.

49 R. Quintana, M. Gosa, D. Jańczewski, E. Kutnyanszky, G. J. Vancso, *Langmuir* **2013**, *29*, 10859–10867.

50 J. S. Dickson, M. Koohmaraie, *Appl. Environ. Microb.* **1989**, *55*, 832–836.

51 E. R. Holm, *Integr.Comp. Biol.* **2012**, *52*, 348–355.

52 R. Holland, T. M. Dugdale, R. Wetherbee, A. B. Brennan, J. A. Finlay, J. A. Callow, M. E. Callow, *Biofouling* **2004**, *20*, 323–329.

53 N. Schwierz, D. Horinek, S. Liese, T. Pirzer, B. N. Balzer, T. Hugel, R. R. Netz, *J. Am. Chem. Soc.* **2012**, *134*, 19628–19638.

54 J. Zheng, L. Y. Li, H. K. Tsao, Y. J. Sheng, S. F. Chen, S. Y. Jiang, *Biophys. J.* **2005**, *89*, 158–166.